The EMBO Journal Vol.17 No.18 pp.5497–5508, 1998

Homologous recombination and non-homologous end-joining pathways of DNA double-strand break repair have overlapping roles in the maintenance of chromosomal integrity in vertebrate cells

Minoru Takata, Masao S.Sasaki[1], Eiichiro Sonoda, Ciaran Morrison, Mitsumasa Hashimoto[2], Hiroshi Utsumi[2], Yuko Yamaguchi-Iwai, Akira Shinohara[3] and Shunichi Takeda[4]

Department of Molecular Immunology and Allergology, Kyoto University Medical School, Konoe Yoshida, Sakyo-ku, Kyoto 606-8315, [1]Radiation Biology Center, Kyoto University, Yoshida Konoe, Sakyo-ku, Kyoto 606-8315, [2]Research Reactor Institute, Kyoto University, Kumatori-cho Noda, Sennan-gun, Osaka 590-04 and [3]Department of Biology, Graduate School of Science, Osaka University, Toyonaka, Osaka 560, Japan

[4]Corresponding author
e-mail: stakeda@mfour.med.kyoto-u.ac.jp

Eukaryotic cells repair DNA double-strand breaks (DSBs) by at least two pathways, homologous recombination (HR) and non-homologous end-joining (NHEJ). Rad54 participates in the first recombinational repair pathway while Ku proteins are involved in NHEJ. To investigate the distinctive as well as redundant roles of these two repair pathways, we analyzed the mutants *RAD54*$^{-/-}$, *KU70*$^{-/-}$ and *RAD54*$^{-/-}$/*KU70*$^{-/-}$, generated from the chicken B-cell line DT40. We found that the NHEJ pathway plays a dominant role in repairing γ-radiation-induced DSBs during G_1–early S phase while recombinational repair is preferentially used in late S–G_2 phase. *RAD54*$^{-/-}$/*KU70*$^{-/-}$ cells were profoundly more sensitive to γ-rays than either single mutant, indicating that the two repair pathways are complementary. Spontaneous chromosomal aberrations and cell death were observed in both *RAD54*$^{-/-}$ and *RAD54*$^{-/-}$/*KU70*$^{-/-}$ cells, with *RAD54*$^{-/-}$/*KU70*$^{-/-}$ cells exhibiting significantly higher levels of chromosomal aberrations than *RAD54*$^{-/-}$ cells. These observations provide the first genetic evidence that both repair pathways play a role in maintaining chromosomal DNA during the cell cycle.

Keywords: homologous recombination/Ku/non-homologous end-joining/Rad54/spontaneous chromosomal break

Introduction

DNA repair is essential for the successful maintenance and propagation of genetic information. Chromosomal double-strand breaks (DSBs) may occur spontaneously and can be induced by DNA damage. In eukaryotes, two DSB repair pathways have been identified that differ in their requirements for DNA homology. DSB repair by homologous recombination (HR) results in the precise repair of the DNA lesion but requires the presence of homologous sequences elsewhere in the genome (e.g. a homologous chromosome or a sister chromatid). This is the primary mechanism of DSB repair in yeast species. In contrast, it has been speculated that vertebrate cells may appear to favor a non-homologous DNA end-joining (NHEJ) pathway for DSB repair because all DSB-repair defective mutant clones analyzed to date have been found to be defective in NHEJ (Weaver, 1995). The NHEJ pathway joins the two ends of a DSB through a process that is largely independent of terminal DNA sequence homology and that therefore produces junctions that can vary in their sequence composition.

The three subunits of DNA-dependent protein kinase (DNA-PK) (Jeggo, 1997), the *XRCC4* gene product (Li *et al*., 1995) and DNA ligase IV (Critchlow *et al*., 1997; Grawunder *et al*., 1997; Wilson *et al*., 1997) are necessary for the NHEJ pathway. The DNA binding subunit of DNA-PK, Ku, is a heterodimer consisting of 70 and 80 kDa subunits (Ku70 and Ku80, respectively) (Mimori and Hardin, 1986; Mimori *et al*., 1990; Yaneva *et al*., 1997). Cells defective in either Ku70 or Ku80 are ionizing-radiation-sensitive and do not complete V(D)J recombination (Smider *et al*., 1994; Taccioli *et al*., 1994; Nussenzweig *et al*., 1996; Zhu *et al*., 1996; Gu *et al*., 1997; Ouyang *et al*., 1997). *Saccharomyces cerevisiae* contains homologues of the Ku70, Ku80 and ligase IV genes, which also play a role in repairing induced DSBs (Feldmann and Winnacker, 1993; Boulton and Jackson, 1996a,b; Milne *et al*., 1996; Teo and Jackson, 1997).

Studies in *S.cerevisiae* have defined the *RAD52* epistasis group of genes, which is believed to represent a pathway for the repair of DSBs by homologous DNA recombination (Game and Mortimer, 1974; reviewed in Petes *et al*., 1991; Game, 1993; Shinohara and Ogawa, 1995). Among the known members of the *RAD52* group, the *RAD51*, *RAD52* and *RAD54* genes are placed in a subgroup because the corresponding mutants possess similar phenotypes; the inactivation of these genes renders *S.cerevisiae* cells highly sensitive to ionizing radiation and methyl methanesulfonate (MMS), both of which induce DSBs, and strongly reduces spontaneous as well as induced mitotic recombination frequencies (Saeki *et al*., 1980). Recently, vertebrate homologues of the *RAD51*, *RAD52* and *RAD54* genes of *S.cerevisiae* have been cloned (Bezzubova *et al*., 1993a,b; Morita *et al*., 1993; Shinohara *et al*., 1993; Kanaar *et al*., 1996). Both chicken B lymphocytes and mouse embryonic stem (ES) cells lacking Rad54 are more sensitive to ionizing radiation than wild-type cells, suggesting that the repair function of the *RAD52* epistasis group genes is conserved throughout evolution (Bezzubova *et al*., 1997; Essers *et al*., 1997).

To study the roles of Rad54-dependent HR repair and Ku-dependent NHEJ pathways, we generated *RAD54*$^{-/-}$, *KU70*$^{-/-}$ and *RAD54*$^{-/-}$/*KU70*$^{-/-}$ clones from the chicken B lymphocyte line DT40 (Baba *et al*., 1985; Buerstedde

Fig. 1. Amino acid sequence comparison between the chicken (GdKu70), human (HsKu70) and murine (MmKu70) Ku70 proteins. Amino acid sequence is shown by the single-letter code. Identical amino acids are shaded. The comparison was made using the Clustal method of the Lasergene Navigator (DNASTAR, Inc., Madison, WI). It should be noted that the chicken *KU70* gene (DDBJ/EMBL/GenBank accession No. AB016529) still retains a methionine at the position where the other genes start. The base sequence around this methionine codon is GCCATGG, while that around the initiation codon is GTGATGG. Thus, both ATG sequence contexts are in accordance with the optimal translation initiation consensus determined by Kozak (1986, 1995).

et al., 1990). The high level of homologous recombination in DT40 cells (Buerstedde and Takeda, 1991; Takeda *et al*., 1992; Bezzubova and Buerstedde, 1994) allows the targeted disruption of two genes in a single cell. The remarkably stable phenotype of parental DT40 cells enables us to compare quantitatively the phenotypes of mutant clones of various genes. Since genetic studies in yeast have shown that the HR and NHEJ pathways act independently while having overlapping roles in repairing induced DSBs (Boulton and Jackson, 1996a,b; Milne *et al*., 1996), we compared the phenotype of *RAD54*$^{-/-}$/*KU70*$^{-/-}$ cells with that of either *RAD54*$^{-/-}$ or *KU70*$^{-/-}$ cells. To study the phenotypes of these mutants, we measured the frequencies of spontaneous and γ-radiation-induced cytogenetic aberrations along with survival following γ-radiation. Our data show that the HR and NHEJ pathways are partially complementary with each other in maintaining chromosomal DNA during the cell cycle as well as in repairing DSBs induced by γ-radiation. In addition, while HR is preferentially used at any stage in the cell cycle to repair DSBs in yeast, it does not necessarily function prior to DNA replication in DT40 cells.

Results

Isolation of the chicken Ku70 cDNA

A cDNA fragment encoding a chicken Ku70 homologue was isolated from a chicken intestinal mucosa cDNA library. An open reading frame in the cDNA clone showed ~70% homology in amino acid sequence to the human Ku70 protein (Feldmann and Winnacker, 1993). An 18 amino acid stretch appears to be appended to the N-terminus in the deduced amino acid sequence of chicken Ku70 (Figure 1, GdKu70); Western blot analysis revealed that chicken Ku70 is slightly larger than human Ku70 (data not shown). Southern blot analysis of chicken genomic DNA showed a single band hybridizing to a chicken Ku cDNA probe (data not shown), indicating that there is a single *KU70* gene in the chicken genome.

KU70 targeting constructs and generation of Ku70-deficient and Rad54/Ku70-doubly deficient DT40 clones

A chicken *KU70* cDNA probe was used to isolate genomic clones of the *KU70* locus, which were partially sequenced to determine the positions of exons. To generate *KU70* deletion constructs, either the histidinol (his) or blasticidin (bsr) resistance gene was inserted between sequences of 1.6 and 3.3 kb in length from the *KU70* locus as shown in Figure 2A. Targeted integration of these constructs was expected to delete amino acids 66–134, and targeting events were defined by the presence of a 2.8 kb band after Southern blot analysis of *Eco*RI-digested genomic DNA hybridized to an external probe (Figure 2A and B).

The KU70–his construct was transfected into wild-type DT40 cells and drug resistant clones were examined by Southern blot analysis to isolate heterozygous *KU70*$^{+/-}$ mutant clones. One of the *KU70*$^{+/-}$ mutant clones was then transfected with the bsr construct to isolate homozygous *KU70*$^{-/-}$ mutant clones. The disruption of the *KU70* gene was verified by Northern and Western blot analyses (Figure 2C and D). To generate *RAD54*$^{-/-}$/*KU70*$^{-/-}$ clones, two *RAD54* deletion constructs were sequentially transfected into a *KU70*$^{-/-}$ clone. The disruption of the *RAD54* gene was verified by Northern blot (data not shown), as described previously (Bezzubova *et al*., 1997).

A substantial fraction of RAD54$^{-/-}$ *and Rad54*$^{-/-}$/*Ku70*$^{-/-}$ *cells die during the cell cycle*

The proliferative properties of wild-type, *RAD54*$^{-/-}$, *KU70*$^{-/-}$ and *RAD54*$^{-/-}$/*KU70*$^{-/-}$ clones were monitored by growth curves and by cell-cycle analysis. The number of cells was counted every 24 h, while maintaining the density of cells at an optimal level (10^5–10^6 cells/ml) (Figure 3A). Wild-type and *KU70*$^{-/-}$ cells proliferated at a significantly higher rate than *RAD54*$^{-/-}$ and *RAD54*$^{-/-}$/*KU70*$^{-/-}$ cells. The plating efficiencies of cells in methylcellulose plates were virtually 100% for wild-type and *KU70*$^{-/-}$, ~80% for *RAD54*$^{-/-}$ and ~50% for *RAD54*$^{-/-}$/*KU70*$^{-/-}$ cells.

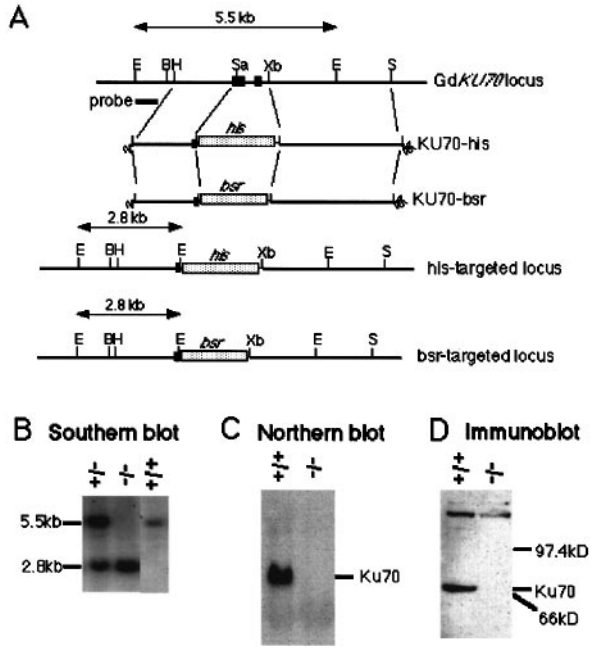

Fig. 2. Generation of *KU70*$^{-/-}$ clones. (**A**) Schematic representation of partial restriction map of the GdKU70 locus, the two gene disruption constructs and the configuration of the targeted loci. Black boxes indicate the positions of exons that were disrupted. Relevant restriction enzyme sites are shown as follows: E, *Eco*RI; B, *Bam*HI; H, *Hin*dIII; Sa, *Sal*I; Xb, *Xba*I; S, *Sac*I. (**B**) Southern blot analysis of wild-type (+/+), heterozygous mutant (+/–) and homozygous mutant (–/–) clones. *Eco*RI-digested genomic DNA was hybridized with the probe DNA shown in (A). (**C**) Northern blot analysis of total RNA (20 μg/lane) of the indicated genotype after hybridization with a chicken Ku70 cDNA probe. (**D**) Western blot analysis of chicken Ku70 expression. Cell extracts were separated by SDS–PAGE, and transferred to a filter. Ku70 was visualized by incubation with rabbit anti-chicken Ku70 serum and subsequent binding of a labeled second antibody.

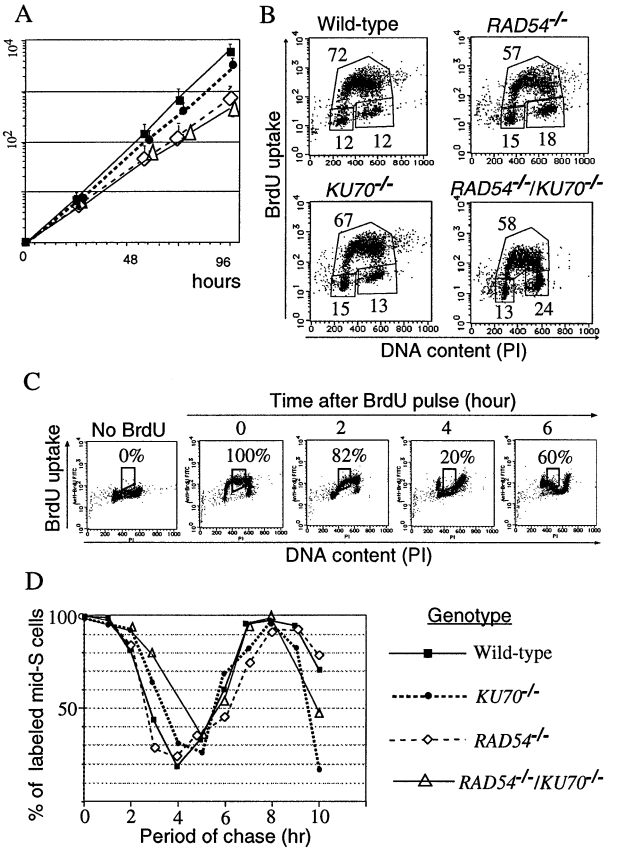

Fig. 3. Proliferative characteristics of wild-type, *KU70*$^{-/-}$, *RAD54*$^{-/-}$ and *KU70*$^{-/-}$/*RAD54*$^{-/-}$ cells. (**A**) Growth curves corresponding to the indicated cell cultures. The genotypes are as displayed at the bottom. Data shown are the average of the results from two separate clones for each genotype. Error bars show the standard deviation of the mean for three experiments. (**B**) Representative cell-cycle distribution of the indicated cell cultures as measured by BrdU incorporation and DNA-content in flow cytometry analysis. Cells were pulse-labeled for 10 min, and subsequently were stained with FITC-anti-BrdU to detect BrdU incorporation (vertical axis, log scale) and propidium iodide to detect total DNA (horizontal axis, linear scale). The upper gate identifies cells incorporating BrdU (approximately S phase), the lower-left gate identifies G_1 cells and the lower-right gate displays G_2–M cells. Numbers show the percentages of cells falling in each gate. (**C**) A representative analysis of the kinetics of progression of wild-type cells through the stages of the cell cycle. S phase cells were labeled using a 10 min pulse of BrdU. The transit of labeled cells through the cell cycle was followed by measuring the percentage of cells in the gate indicated with time after BrdU pulse-labeling (time zero). The relative percentages of cells in the gate were calculated as the percentage of cells falling in the box at each time divided by the percentage of cells falling in the box at time zero ×100 (%). (**D**) The calculated relative percentages of each type of cells are plotted with time. The symbols for each sample are shown on the right. The progression of BrdU-labeled (i.e. S phase) cells out of S phase, and into first G_2–M (4n DNA content), then G_1 (2n DNA content), and back into S phase was very similar between the four types of cells and took ~8 h.

Pulse-labeling of asynchronous cells with bromodeoxyuridine (BrdU) showed that the proportion of *RAD54*$^{-/-}$ and *RAD54*$^{-/-}$/*KU70*$^{-/-}$ cells in G_2–M phase was significantly larger than that of wild-type cells: 14.7 ± 2.5% for wild-type, 14.7 ± 2.1% for *KU70*$^{-/-}$, 18.3 ± 1.5% for *RAD54*$^{-/-}$ and 23.0 ± 4.4% for *RAD54*$^{-/-}$/*KU70*$^{-/-}$ cells (Figure 3B). The length of a single cell cycle was measured in a pulse–chase experiment. After a 10 min pulse of BrdU, we followed the progression of BrdU-labeled S phase cells throughout the cell cycle, measured by DNA content analysis (Figure 3C). The progression of the four types of culture out of S phase, and into first G_2–M (4n DNA content), and then G_1 (2n DNA content), was very similar, a single cell cycle taking ~8 h (Figure 3D). This conclusion is in agreement with our cell-cycle analyses following synchronization with nocodazole, which synchronizes cells at prometaphase by blocking the assembly of mitotic spindles (Figure 6B).

Given that the lengths of a single cell cycle of wild-type, *RAD54*$^{-/-}$ and *RAD54*$^{-/-}$/*KU70*$^{-/-}$ cells were essentially the same, the lower rates of proliferation of *RAD54*$^{-/-}$/*KU70*$^{-/-}$ and *RAD54*$^{-/-}$ cell cultures seemed likely to be caused by elevated levels of spontaneous cell death. The fraction of spontaneous cell death of the *RAD54*$^{-/-}$ clones during a single cell cycle is calculated as 13%, as described in Materials and methods. The fraction of dead cells in the slower-proliferating cell cultures was analyzed using flow cytometry (Figure 4). In flow cytometric analyses, dead cells were expected to be smaller in size and to show bright propidium iodide (PI) staining. In addition, a substantial number of PI dull-positive cells were found in the *RAD54*$^{-/-}$/*KU70*$^{-/-}$ culture. They were annexin-V positive (Martin *et al*., 1995; Uckun *et al*., 1996) (Figure 4, upper histogram), suggesting that they were undergoing apoptosis. Thus, we assessed the percentage of dead and dying cells by measuring the cells falling in the

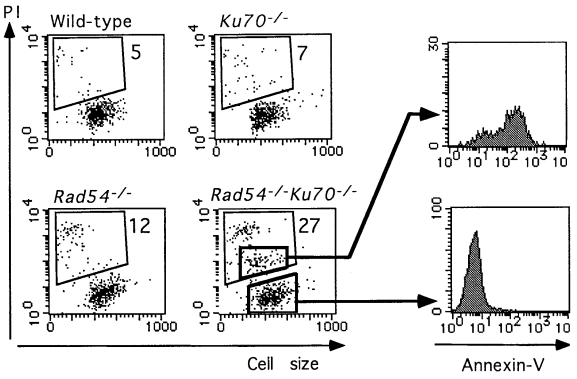

Fig. 4. Spontaneous cell death in *RAD54*$^{-/-}$ and *KU70*$^{-/-}$/*RAD54*$^{-/-}$ DT40 cells. Representative dot plots display the size (forward scatter) on the *x* axis (linear scale) and the intensity of PI staining on the *y* axis (log scale). Numbers indicate the percentages of dying and dead cells, which are PI^{dull} and PI^{bright}. From three separate experiments, the mean percentage and standard deviation of dead and dying cells was 5.9 ± 0.8 for wild-type, 8.7 ± 2.1 for *RAD54*$^{-/-}$, 12 ± 3 for *RAD54*$^{-/-}$ and 22 ± 6.9 for *RAD54*$^{-/-}$/*KU70*$^{-/-}$ cells. PI^{dull} and PI^{-} *KU70*$^{-/-}$/*RAD54*$^{-/-}$ cells were further analyzed by staining with Annexin V as shown in histograms (top, PI^{dull} population; bottom, PI^{-} population).

PI^{dull}/PI^{bright} gate of the dot plots as shown in Figure 4. This analysis revealed that more dead as well as dying cells were present in *RAD54*$^{-/-}$/*KU70*$^{-/-}$ and *RAD54*$^{-/-}$ cell cultures than in wild-type, with only a slightly elevated lethality in the absence of Ku70 alone.

Increased levels of spontaneous chromosomal aberrations in RAD54$^{-/-}$ *and RAD54*$^{-/-}$/*KU70*$^{-/-}$ *cells but not in KU70*$^{-/-}$ *cells*

The presence of a single unrepaired DSB is sufficient to induce cell death in yeast, as shown by the inducible expression of the HO nuclease in radiation-sensitive yeast mutants (Game, 1993). Given the role of both Rad54- and Ku-dependent pathways in DSB repair, the cell death of *RAD54*$^{-/-}$ and *RAD54*$^{-/-}$/*KU70*$^{-/-}$ cells suggests that both pathways may repair spontaneously occurring DSBs in chromosomal DNA during the cell cycle. To test this hypothesis, we performed chromosome analysis of metaphase-arrested cells. DT40 cells display a stable karyotype with a modal chromosome number of 80 in total, which comprises 11 autosomal macrochromosomes, the ZW sex chromosomes and 67 microchromosomes (Sonoda *et al*., 1998). Since alterations in the minichromosomes are difficult to assess, subsequent analysis of chromosome structural aberrations was limited to the 11 autosomal macrochromosomes and the Z chromosome in conventionally Giemsa-stained metaphase cells. Following the screening criteria of ISCN (ISCN1985, 1985), chromosomal aberrations were defined as isochromatid-type when both sister chromatids of a single chromosome were broken at the same locus, while defined as chromatid-type when a single chromatid was broken.

KU70$^{-/-}$ and wild-type cells exhibited very few chromosomal aberrations (Table I), in agreement with previous observations (Kemp and Jeggo, 1986; Darroudi and Natarajan, 1987). In marked contrast, *RAD54*$^{-/-}$ clones frequently displayed chromatid-type breaks. Interestingly, *RAD54*$^{-/-}$/*KU70*$^{-/-}$ cells contained more chromosomal aberrations than *RAD54*$^{-/-}$ cells, although *KU70*$^{-/-}$ cells did not exhibit an increased level of chromosomal aberrations. Thus, Rad54-dependent HR may prevent chromosomal aberrations while Ku70 may function as a back-up for the Rad54-dependent pathway in vertebrate cells. The presence of spontaneous chromosomal aberrations in cells defective in DNA repair supports the notion that genomic DNA lesions may occur spontaneously during the cell cycle and that unrepaired DSBs lead to apoptotic cell death of *RAD54*$^{-/-}$ and *RAD54*$^{-/-}$/*KU70*$^{-/-}$ clones. This observation shows for the first time that NHEJ also can contribute to the maintenance of chromosomal integrity in higher eukaryotic cells.

Synergistic increase in sensitivity to genotoxic damage with mutations in Ku70 and Rad54

The repair capacity of cells defective in Rad54 and/or Ku70 was analyzed in a colony survival assay (Figure 5). *RAD54*$^{-/-}$ cells were highly sensitive to ionizing irradiation (Figure 5A and C) and MMS (Figure 5D), as previously reported (Bezzubova *et al*., 1997). *RAD54*$^{-/-}$/*KU70*$^{-/-}$ cells were more sensitive to ionizing radiation and MMS than either single mutant, and expression of either chicken Rad54 or Ku70 in *RAD54*$^{-/-}$/*KU70*$^{-/-}$ cells restored DNA repair activities to those of the respective single mutant levels (Figure 5B). Thus, the two repair pathways may partially complement each other in repairing induced DSBs in DT40 cells. The higher sensitivity of *RAD54*$^{-/-}$ than *KU70*$^{-/-}$ cells to ionizing radiation indicates that HR is preferentially used to repair induced DSBs while NHEJ can repair DSBs as a back-up for HR, as has been observed in yeast cells (Winnacker, 1993; Boulton and Jackson, 1996a,b; Feldmann and Milne *et al*., 1996; Teo and Jackson, 1997). In contrast to previous reports on the effects of the absence of Ku70/80 (Jeggo, 1990; Zdzienicka, 1995; Gu *et al*., 1997; Ouyang *et al*., 1997), *KU70*$^{-/-}$ DT40 cells were somewhat less sensitive to genotoxic treatments than wild-type cells, at higher doses of ionizing radiation and MMS treatments.

The recombinational repair pathway functions during late S–G$_2$ *phase while the NHEJ pathway is preferentially used during G1–early S phase*

To further dissect the roles of the two repair pathways, we irradiated synchronized cells and analyzed their sensitivity to γ-radiation at each stage of the cell cycle. Following the treatment of cells with nocodazole for seven hours, most cells accumulated in G_2–M phase (Figure 6A). By 9.5 h after the removal of nocodazole, some cells had begun a second round of the cell cycle. After synchronization of *RAD54*$^{-/-}$ and *KU70*$^{-/-}$ cells, their cell-cycle progression was indistinguishable from that of wild-type cells (Figure 6B). A substantial number of *RAD54*$^{-/-}$/*KU70*$^{-/-}$ cells were found to die following synchronization.

After release from nocodazole treatment, cells were γ-irradiated at various time points and subsequently seeded on methylcellulose plates (Figure 7). The pattern of radiation sensitivity in each stage of the cell cycle was essentially the same in both the first and second round of the cell cycle after synchronization. Consistent with previous reports on cell-cycle and radiation resistance (Jeggo, 1990, 1997), wild-type DT40 cells showed increased radiation resistance in late S–G_2 phase relative

Table I. Spontaneous chromosomal aberrations

Genotype	Isochromatid		Chromatid		Exchanges[a]	Total aberrations[b] (per cell ± SE[c])
	Breaks[a]	Gaps[a]	Breaks[a]	Gaps[a]		
Wild-type	0.25	0.25	0.25	1.25	0	0.02 ± 0.007
KU70$^{-/-}$	0	0	0.5	0.5	0	0.01 ± 0.007
RAD54$^{-/-}$ #1	1	1	3	2.7	0	0.077 ± 0.016
RAD54$^{-/-}$ #2	0.33	0.67	3	1	0.67	0.057 ± 0.014
KU70$^{-/-}$/*RAD54*$^{-/-}$	1.7	0.83	4.5	3	0.5	0.11 ± 0.01

Cells were treated with colcemid for 3 h to enrich mitotic cells. The actual number of cells analyzed was 400 for wild-type, 200 for *KU70*$^{-/-}$, 300 each for *RAD54*$^{-/-}$ #1 and #2, and 600 for *KU70*$^{-/-}$/*RAD54*$^{-/-}$ cells.

[a]Data are presented as the number of aberrations per 100 cells.

[b]The total number of chromosomal aberrations.

[c]If the numbers of cells analyzed and total chromosomal aberrations are defined as N and x, respectively, the number of total aberrations per cell ± SE is calculated as $x/N \pm \sqrt{x}/N$, based on the Poisson distribution of spontaneous chromosomal aberrations we observed previously (Sonoda *et al.*, 1998).

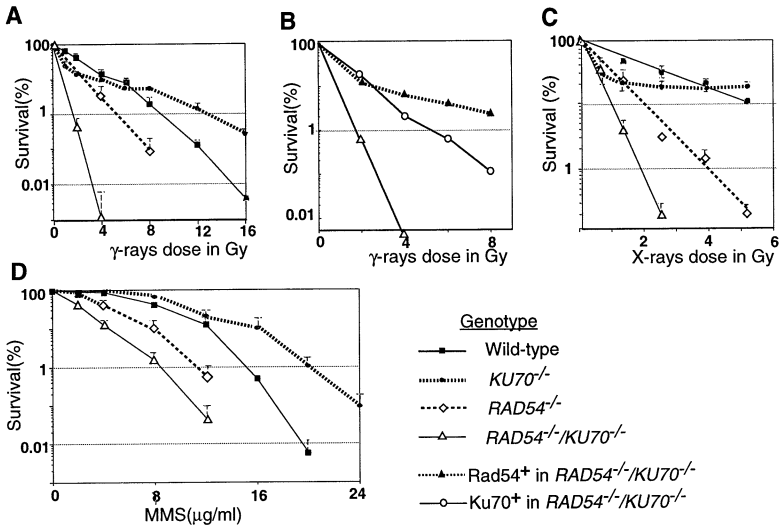

Fig. 5. Graphs displaying the ionizing radiation and the MMS sensitivity of asynchronous clones of the various genotypes indicated. (**A** and **B**) The fractions of colonies surviving after γ-radiation compared to non-irradiated controls of the same genotype are shown on the *y* axis in a logarithmic scale. The radiation doses are displayed on the *x* axis in a linear scale. (B) *RAD54*$^{-/-}$/*KU70*$^{-/-}$ clones were reconstituted with either chicken RAD54 or KU70 cDNA. Data from a representative clone of each type of the reconstituted cells are shown. (**C**) The fractions of colonies surviving after X-radiation. (**D**) The fractions of surviving colonies and the MMS concentrations are displayed on the *y* and *x* axes, respectively. The genotypes are as indicated at right bottom. (A, C and D) Data shown are the average of the results from two separate clones of each genotype. Error bars show the standard deviation of the mean for at least three separate experiments.

to G_1–early S phase. In contrast to wild-type DT40 cells, *RAD54*$^{-/-}$ cells did not show increased radiation resistance in late S–G_2 phase (Figure 7). This observation implies that the Rad54-dependent recombinational repair pathway may function after a pair of sister chromatids are generated by DNA replication. Such a relatively flat response of radiosensitivity throughout the cell cycle was also observed in a mammalian cell line deficient in Xrcc2, which is a distant homologue of Rad51 and may be involved in recombinational repair (Cheong *et al.*, 1994; Thompson, 1996; Liu *et al.*, 1998).

KU70$^{-/-}$ cells exhibited a remarkably elevated sensitivity to γ-ray irradiation in G_1–early S phase (Figure 7), as observed in mammalian cell lines deficient in the NHEJ pathway (Stamato *et al.*, 1988; Jeggo, 1990; Lee *et al.*, 1997). This elevated sensitivity was also observed in the second round of the cell cycle, although the extent of synchronization is reduced compared with the first round of the cell cycle (Figure 6A). The elevated sensitivity of *KU70*$^{-/-}$ cells synchronized in G_1–early S phase to γ-rays is consistent with the elevated sensitivity of asynchronous *KU70*$^{-/-}$ cells to lower doses (up to 2 Gy) of ionizing irradiation (Figure 5A and C).

To confirm the results obtained from the synchronization with nocodazole, we also employed elutriation to enrich cells at G_1 phase (Figure 8A). Following the incubation of the cells at 39.5°C, they underwent a round of the cell cycle in a synchronous manner (Figure 8B). Synchronized cells were subsequently irradiated with X-rays at various time points, and their radiosensitivity was analyzed in the same manner as in Figure 7. The pattern of radiosensitivity of wild-type, *RAD54*$^{-/-}$ and *KU70*$^{-/-}$ cells were essentially the same as observed in the cells following nocodazole treatment for synchronization (Figure 8C).

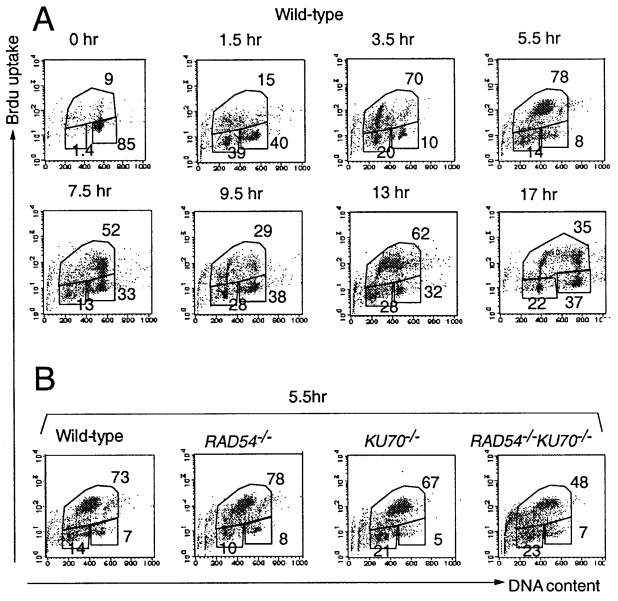

Fig. 6. Synchronization of DT40 cells with nocodazole. At each time point following nocodazole treatment, the progression of the cell cycle was analyzed with flow cytometry in the same manner as in Figure 3B. (**A**) The progression of the cell cycle of wild-type DT40 cells at various time points after nocodazole treatment. (**B**) The cell cycle of the indicated four types of cells progressed in the same manner, as determined at 5.5 h following synchronization. The progression of the cell cycle was the same among the four types of cells until 17 h after synchronization (data not shown).

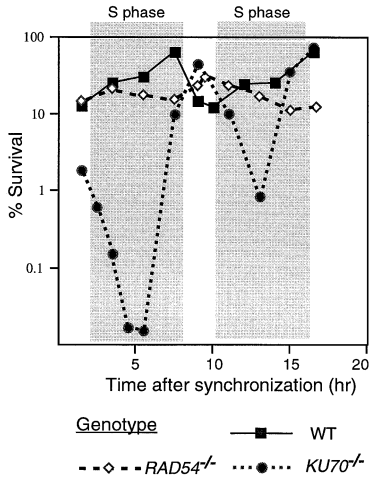

Fig. 7. Cell-cycle stage specific sensitivity to γ-radiation. Cells were treated with 2 Gy γ-radiation at the indicated time points following synchronization. The fractions of colonies surviving after irradiation compared with non-irradiated controls of the same genotype are shown. In shaded areas, most cells were in S phase. 4 Gy γ-radiation also exhibited the same pattern of sensitivities during the cell cycle in each of the genotypes (data not shown).

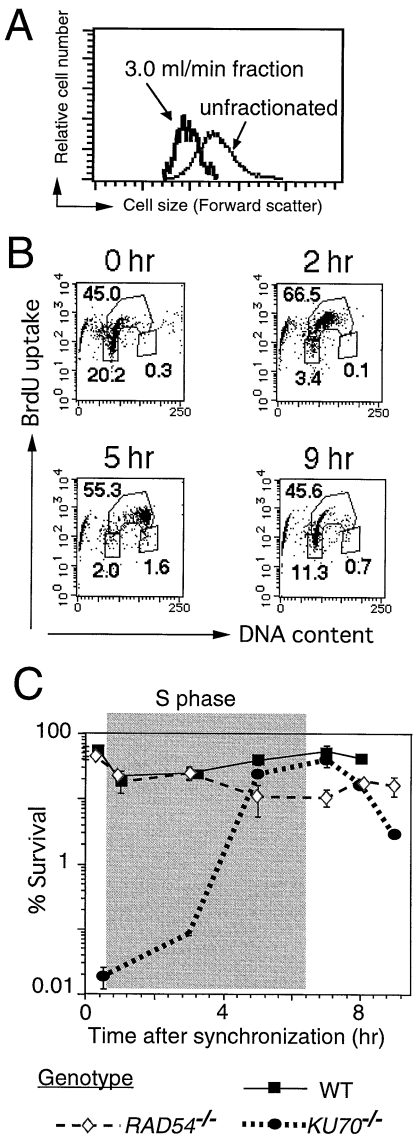

Fig. 8. Cell-cycle stage specific sensitivity to X-radiation following synchronization by elutriation. (**A**) The size of cells separated by elutriation were analyzed with flow cytometry. Only PI^- cells are shown to exclude dead cells. (**B**) Cells separated by elutriation were incubated at 39.5°C, and the progression of the cell cycle was analyzed with 10 min pulse-labeling of BrdU at indicated time points. (**C**) Cells were treated with 2 Gy X-radiation at the indicated time points following synchronization. The fractions of colonies surviving after irradiation compared to non-irradiated controls of the same genotype are shown. Error bars show the standard deviation of the mean for three experiments.

γ-radiation induces elevated levels of chromosomal aberrations in cells deficient in DSB repair

Exponentially growing cultures of wild-type, *KU70*$^{-/-}$ and *RAD54*$^{-/-}$ cells were treated with 2 Gy γ-radiation and sampled at 3, 6, 9 and 12 h after irradiation (Table II, 2 Gy radiation). In addition, *RAD54*$^{-/-}$ and *KU70*$^{-/-}$/*RAD54*$^{-/-}$ cells were treated with 0.8 and 0.3 Gy γ-radiation, respectively, the doses of which were equivalent to 2 Gy on wild-type (LD_{60}). Karyotypic analysis of at least 100 mitotic cells was used to define the integrity of the chromosomes. Cells undergoing mitosis at 0–3 and 6–9 h are expected to have been irradiated mainly in late S–G_2 and G_1–early S phase, respectively. In wild-type cells, the number of chromatid breaks decreased with time following irradiation, which may reflect the rapid repair of DSBs. On the other hand, the level of isochromatid breaks was highest at 6–9 h post-radiation, implying that a broken chromosome was converted to a pair of broken sister chromatids following DNA replication.

The numbers of chromatid breaks were elevated ~10-

Table II. Ionizing radiation-induced chromosomal aberrations

2 Gy radiation Genotype	γ-dose (Gy)	Time (h[a])	Isochromatid		Chromatid		Exchanges[b]	Total aberrations (per cell ± SE[c])
			Breaks[b]	Gaps[b]	Breaks[b]	Gaps[b]		
Wild-type	2	0–3	2.7	4.7	17	1.3	0.7	0.26 ± 0.04
	2	3–6	1.3	4.7	4.7	0.7	0	0.11 ± 0.03
	2	6–9	7.3	2.7	1.3	0.7	1.3	0.13 ± 0.03
	2	9–12	3.3	4	0	1.3	2.7	0.11 ± 0.03
KU70$^{-/-}$	2	0–3	2.5	5	19	7	1	0.35 ± 0.04
	2	3–6	2	5	3	2	1	0.13 ± 0.03
	2	6–9	22	8	12	2	3	0.47 ± 0.07
	2	9–12	9	7	4	5	3	0.28 ± 0.05
RAD54$^{-/-}$	2	0–3	28	2	201	27	23	2.81 ± 0.17
	2	3–6	20	11	72	9	25	1.37 ± 0.12
	2	6–9	15	7	60	6	31	1.19 ± 0.11
	2	9–12	19	4	40	4	35	1.02 ± 0.10
Dose equivalent to 2 Gy on wild-type (LD60)								
RAD54$^{-/-}$	0.8	0–3	8	1	39	5	3	0.56 ± 0.07
	0.8	3–6	6	2	7	4	0	0.19 ± 0.04
	0.8	6–9	3	1	5	6	0	0.15 ± 0.04
	0.8	9–12	2	0	7	1	3	0.13 ± 0.04
KU70$^{-/-}$/*RAD54*$^{-/-}$	0.3	0–3	12	11	130	18	1	1.72 ± 0.13
	0.3	3–6	1	3	59	13	3	0.79 ± 0.09
	0.3	6–9	2	6	8	3	4	0.23 ± 0.05
	0.3	9–12	4	2	3	2	8	0.19 ± 0.04

[a]Cells were treated with colcemid during indicated periods (hours) after γ-irradiation. At least 100 cells were analyzed at each time point.
[b]The number of aberrations per 100 cells is presented.
[c]The number of total aberrations is presented. The number of total aberrations per cell ± SE is calculated as $x/N \pm \sqrt{x}/N$ as in Table I.

fold in *RAD54*$^{-/-}$ cells compared with wild-type cells following 2 Gy irradiation. This observation supports the notion that the HR repair pathway functions after a pair of sister chromatids are generated by DNA replication. Interestingly, 2-Gy irradiated *RAD54*$^{-/-}$ cells displayed slightly elevated levels of isochromatid-type aberrations at every time point. Although the origin of isochromatid-type aberrations is not fully understood, this observation implies that HR may function prior to and/or during DNA replication and that a defect in this repair results in breaks at the same sites in both sister chromatids, i.e. isochromatid breaks. *KU70*$^{-/-}$ cells exhibited a biphasic response to γ-radiation; the number of chromosomal aberrations increased from 3–6 to 6–9 h post-radiation. These observations agree with the extremely high radiation sensitivity of *KU70*$^{-/-}$ cells at G_1–early S phase. The increase in exchanges was comparable among 2-Gy irradiated wild-type, 0.8-Gy irradiated *RAD54*$^{-/-}$, 2-Gy irradiated *KU70*$^{-/-}$ and 0.3-Gy irradiated *RAD54*$^{-/-}$/*KU70*$^{-/-}$ cells, which showed the same levels of breaks and gaps (Table II). Thus, when ionizing irradiation induces DSBs, neither Rad54 nor Ku is necessarily involved in the rejoining events that cause chromatid exchanges.

Discussion

We show that Rad54 and Ku are complementary not only in repair of induced DSBs but also in the maintenance of chromosomal integrity in cycling vertebrate cells. However, RAD54 and Ku act differentially in DSB repair during the cell cycle.

Repair of spontaneous DSBs in cycling vertebrate cells

We found that an elevated level of spontaneous chromosomal breaks occur in *RAD54*$^{-/-}$ DT40 cells, as observed in Rad51-deficient DT40 cells (Sonoda *et al*., 1998). It is known that Rad54 and Rad51 are involved in DSB repair and expressed in cycling but not in resting cells (Bezzubova *et al*., 1993a; Shinohara *et al*., 1993; Tashiro *et al*., 1996; Yamamoto *et al*., 1996). The presence of spontaneous chromosomal breaks in *RAD54*$^{-/-}$ cells therefore indicates that a small number of chromosomal lesions occur during the cell cycle and that the HR pathway is responsible for repairing these lesions.

It remains to be investigated how and what kinds of DNA lesions are generated spontaneously during the cell cycle. A recent report showed that the Holliday junction recombination intermediates accumulate spontaneously during DNA replication in mitotically growing yeast (Zou and Rothstein, 1997). The authors hypothesized that spontaneously occurring DNA lesions, such as nicks, chemical modification and mismatches, are converted to DSBs when a DNA replication fork encounters such a lesion; these DSBs may stimulate the HR pathway, inducing recombinational intermediates between the damaged and intact sister chromatids. Thus, the absence of such HR would result in chromatid breaks, which is in agreement with the appearance of spontaneous chromatid breaks in *RAD54*$^{-/-}$ DT40 cells.

A role for HR in the maintenance of genomic integrity has been inferred from several observations from vertebrate and yeast cells. First, a conditional Rad51 mutant

derived from DT40 showed that most metaphase-arrested Rad51-deficient cells carried a few isochromatid-type breaks which led to cell death (Sonoda *et al*., 1998). Secondly, although yeast species deficient in Rad51 and Rad54 are viable, they grow slowly with poor plating efficiency and a high frequency of chromosome loss (Fingerhut *et al*., 1984; Muris *et al*., 1993, 1996). The chromosome loss seems to be caused by unrepaired chromosomal breaks. Since vertebrate cells carry a much larger genome than yeast cells, a higher incidence of spontaneous DSBs is expected in a single higher eukaryotic cell than in a yeast cell. Accordingly, HR of higher eukaryotes may play a greater role in maintaining chromosomal integrity. Since small numbers of random chromosomal aberrations cannot be identified in yeast cells, our study defines for the first time the role of Rad54 in the maintenance of chromosomal integrity during the cell cycle.

Although the *rad51* and *rad54* mutants in *S.cerevisiae* exhibit similar phenotypes, DT40 clones deficient in Rad51 and Rad54 exhibit different phenotypes: while a Rad51 mutant is lethal, Rad54 mutant cells can proliferate, with a small fraction of the cells dying spontaneously at each cell cycle. Similarly, while the *RAD51* gene is essential for early murine embryonic development (Lim and Hasty, 1996; Tsuzuki *et al*., 1996), *RAD54*$^{-/-}$ mice are viable and fertile (Essers *et al*., 1997). Rad51 and Rad54 may therefore play distinct roles in HR following DNA replication. This is supported by the fact that Rad51-deficient cells display an increased level of isochromatid but not of chromatid breaks. Furthermore, the reported associations of Rad51 with p53 (Sturzbecher *et al*., 1996), Brca1 (Scully *et al*., 1997) and Brca2 (Mizuta *et al*., 1997; Sharan *et al*., 1997) imply that Rad51 may have functions additional to its role in HR. Alternatively, since there exist other structural homologues of the *RAD54* gene in mammals as well as chicken (Gecz *et al*., 1994; Bezzubova *et al*., 1997), such gene products may complement defective Rad54.

Spontaneous chromosomal aberrations were not detected in either mammalian cells deficient in NHEJ (Kemp and Jeggo, 1986; Darroudi and Natarajan, 1987) or in *KU70*$^{-/-}$ DT40 cells. However, the number of spontaneous chromosomal aberrations as well as the spontaneous cell death rate was slightly elevated in *RAD54*$^{-/-}$/*KU70*$^{-/-}$ cells compared with *RAD54*$^{-/-}$ cells. This suggests that the Ku-dependent NHEJ pathway is also involved in the maintenance of chromosomal DNA and that it may act as a back-up of the HR pathway for repairing spontaneously occurring DNA lesions.

Rad54 is important for recombinational repair of a broken chromatid with the intact sister chromatid

DSB repair by homologous recombination requires the presence of homologous sequences elsewhere in the genome, e.g. a homologous chromosome or a sister chromatid. In yeast, the HR pathway can repair induced DSBs by using the other intact homologous chromosome as well as the sister chromatid (Moore and Haber, 1996). On the other hand, the contribution of allelic recombination to induced DSB repair is not clear in vertebrate cells.

Compared with wild-type cells, *RAD54*$^{-/-}$ cells exhibit higher γ-ray sensitivity during late S–G_2 phase (Figure 7) and an increased level of chromatid breaks following γ-ray irradiation (Table II). These findings suggest that the HR pathway involving Rad54 may repair a DSB in a chromatid by using the intact sister chromatid. Recent studies on yeast species showed that there are protein bridges holding sister chromatids together (Guacci *et al*., 1997; Michaelis *et al*., 1997). The close proximity of a pair of sister chromatids may account for the efficient recombinational repair of DSBs during late S–G_2 phase, as has been observed in yeast cells (Kadyk and Hartwell, 1992).

Previous studies showed that the frequency of spontaneous allelic recombination in higher eukaryotic cells appears to be extremely low, of the order of 10^{-8} (Subramani and Seaton, 1988; Benjamin *et al*., 1991; Godwin *et al*., 1994; Moynahan and Jasin, 1997). Furthermore, allelic recombination should be suppressed in vertebrate cells because it may cause loss of heterozygosity and possible tumorigenesis. A recent study showed that the induction of a DSB in the genome by the expression of a restriction enzyme elevated the frequency of allelic recombination by a few hundred fold, implying that induced DSBs can be repaired by allelic recombination (Moynahan and Jasin, 1997). However, this study did not address the relative contribution of allelic recombination to DSB repair. The present study shows that *RAD54*$^{-/-}$ cells did not exhibit increased sensitivity to γ-rays in G_1–early S phase, suggesting that allelic recombination was not primarily employed for the repair of induced DSBs. Furthermore, *KU70*$^{-/-}$ cells exhibited the extremely high sensitivity to ionizing radiation prior to DNA replication suggesting that recombinational repair through heteroallelic recombination may occur only occasionally in DT40, even in the absence of Ku70.

Rad54-dependent recombinational repair may play a more important role in DSB repair in DT40 cells than in murine ES cells

The roles of the two DSB repair pathways appear to be somewhat different between DT40 and mouse ES cells. Although both types of cells undergo the cell cycle with comparable G_1, S and G_2 periods (Savatier *et al*., 1996), a defect in Rad54 increases the γ-ray sensitivity of asynchronous DT40 cells more strongly than that of asynchronous ES cells (Essers *et al*., 1997). Conversely, a defect in Ku70 affects DT40 cells rather less than ES cells (Gu *et al*., 1997). These observations show that the HR pathway is more important for DSB repair in DT40 than in ES cells.

HR can repair DSBs with higher fidelity than the NHEJ pathway, possibly explaining the observed higher survival of *KU70*$^{-/-}$ cells than wild-type cells when asynchronous cells were treated with either higher doses of ionizing radiation (Figure 5A and C) or MMS (Figure 5D). The higher doses of genotoxic treatments would allow only the most resistant fraction of the treated cells to survive, thereby measuring the sensitivity of cells at late S to G_2 phase. At this phase, the recombinational repair pathway alone can repair DSBs very efficiently in DT40 cells. This may explain the presence of Ku70 does not necessarily cause a decrease in the number of lethal unrepaired DSBs. Rather, NHEJ activity may actually result in an increase

in lethal mutation following genotoxic treatment because of its lower fidelity than recombinational repair.

The preferential usage of HR over NHEJ in DT40 for DSB repair is consistent with the finding that the ratios of targeted to random integration in DT40 are much higher than in any other vertebrate cells, including ES cells (Buerstedde and Takeda, 1991; Bezzubova and Buerstedde, 1994). Alternatively, the relative activity of Rad54 over the other Rad54-related proteins (Gecz *et al*., 1994; Bezzubova *et al*., 1997) in DT40 might be higher than in ES cells, explaining the more pronounced phenotype of *RAD54*$^{-/-}$ DT40 as compared with *RAD54*$^{-/-}$ ES clones. In fact, although targeted integration events were hardly detectable in *RAD54*$^{-/-}$ DT40 cells (Bezzubova *et al*., 1997), the frequency of targeted integration was only several-fold reduced in *RAD54*$^{-/-}$ ES cells (Essers *et al*., 1997). Thus, targeted integration in ES cells may occur independently of Rad54.

The present data on the two DSB repair pathways are consistent with previous studies on mammalian mutant cell lines (Stamato *et al*., 1988; Jeggo, 1990; Cheong *et al*., 1994; Thompson, 1996; Lee *et al*., 1997; Liu *et al*., 1998). In addition, the phenotypes of the following DT40 mutants are very similar to the corresponding murine ES mutants: lethality of Rad51-deficient cells (Tsuzuki *et al*., 1996; Sonoda *et al*., 1998), apparently normal radiosensitivity of Rad52-deficient cells (Rijkers *et al*., 1998; Yamaguchi-Iwai *et al*., 1998), and increased radiosensitivity of Rad54-deficient cells (Bezzubova *et al*., 1997; Essers *et al*., 1997). These observations indicate that DT40 is indeed a suitable model system to study HR in higher eukaryotic cells.

Materials and methods

Construction of the targeting and expression vectors and generation of antisera

Chicken Ku70 partial cDNA clone was obtained by screening a chicken spleen cDNA library (Clontech, Palo Alto, CA) with a human Ku70 cDNA fragment (kindly provided by Dr Mimori, Keio University, Tokyo, Japan) under conditions of low stringency. Using this cDNA fragment, chicken Ku70 full-length cDNA and genomic DNA were isolated from a chicken intestinal mucosa cDNA library (Clontech) and liver genomic library (Stratagene, La Jolla, CA), respectively. Identity of the clones was confirmed by sequencing. Chicken *KU70* disruption constructs, KU70–his and KU70–bsr, were made by replacing ~1 kb *Sal*I–*Xba*I genomic sequence with his- or bsr-selection marker cassettes (Takata and Kurosaki, 1996; Bezzubova *et al*., 1997). The previously described chicken RAD54 targeting constructs, RAD54–his and RAD54–neo (Bezzubova *et al*., 1997), were modified by replacing his with a hygro cassette (Buerstedde and Takeda, 1991) and neo with a puro cassette (Sugawara *et al*., 1997), resulting in the construction of RAD54–hygro and RAD54–puro, respectively. To make the Rad54 expression construct, the full-length chicken Rad54 cDNA was inserted into pAneo vector (Sugawara *et al*., 1997). A glutathione *S*-transferase (GST) fusion construct containing a part of chicken *KU70* (amino acids 472–577) was made by cloning a PCR fragment from chicken Ku70 cDNA into pGEX-3X (Pharmacia, Uppsala, Sweden). The resulting fusion protein was purified by glutathione–Sepharose 4B column (Pharmacia), and injected into a rabbit to raise anti-chicken Ku70 antisera.

Gene targeting and cell culture

Cells were cultured in RPMI#1640 medium supplemented with 10^{-5} M β-mercaptoethanol, penicillin, streptomycin, 10% fetal calf serum and 1% chicken serum (Sigma, St Louis, MO) at 39.5°C. For gene targeting of the chicken *KU70* locus, 10^7 DT40 cells were suspended in 0.5 ml phosphate-buffered saline (PBS) containing 30 μg of linearized targeting vector KU70–his and electroporated with a Gene Pulser apparatus (Bio-Rad, Hercules, CA) at 550 V and 25 μF. Following electroporation, cells were transferred to 40 ml fresh medium and incubated for 24 h. Cells were then resuspended in ~80 ml medium containing 1 mg/ml histinidol (Sigma) and divided into four 96-well plates. After 7–10 days, drug resistant colonies were transferred to 24-well plates. Genomic DNA was extracted from each expanded clone by standard procedures, and clones that had undergone targeted recombination were identified by Southern blot analysis. A his-targeted clone was further transfected with KU70–bsr, and selected in medium containing 25 μg/ml blasticidin-S (Calbiochem, La Jolla, CA). To make *KU70*$^{-/-}$/*RAD54*$^{-/-}$ doubly targeted clone, the *KU70*$^{-/-}$ clone was sequentially transfected with RAD54–hygro and RAD54–puro as above. Clones were selected in medium containing 2.5 mg/ml hygromycin (Calbiochem) after the first transfection, and then both hygromycin and 0.5 μg/ml puromycin (Sigma) after the second transfection.

Western and Northern blot analysis

10^6 cells were washed with PBS and lysed in 20 μl SDS lysis buffer (25 mM Tris–HCl pH 6.5, 1% SDS, 0.24 M β-mercaptoethanol, 0.1% Bromophenol Blue, 5% glycerol). Following sonication and boiling, aliquots (routinely 50%) were subjected to 10% SDS–PAGE. After transfer to a nylon membrane, proteins were detected by polyclonal rabbit anti-chicken Ku70 serum and HRP-conjugated goat anti-rabbit Ig (Amersham, Buckinghamshire, England) using Super Signal™ CL-HRP Substrate System (Pierce, Rockford, IL). For Northern blot analysis, ~10^7 cells were washed once with PBS and total RNA was extracted using Tri-sol (Gibco-BRL, Grand Island, NY). RNA (20 μg/lane) was separated in 1.2% formaldehyde gel, transferred to a nylon membrane, and hybridized with ^{32}P-labeled chicken Rad54 or Ku70 cDNA fragment.

Cell counting and cell-cycle analysis

Cell numbers were determined by mixing PI-stained sample with a fixed number of 25 μ microspheres (Polysciences Inc., Warrington, PA), which can be distinguished from cells by forward and side scatter characteristics during flow cytometric analysis. The number of beads and viable cells were counted simultaneously as gated events, and cell numbers were calculated. We analyzed the growth curve of each clone at least three times. For cell-cycle analyses, cells were labeled for 10 min with 20 μM BrdU (Amersham). They were then harvested and fixed at 4°C overnight with 70% ethanol, and successively incubated as follows: (i) in 4N HCl, 0.5% Triton X-100 for 30 min at room temperature; (ii) in FITC-conjugated anti-BrdU antibody (Pharmingen, San Diego, CA) for 1 h at room temperature; (iii) in 5 μg/ml PI in PBS. Between each incubation, cells were washed with PBS containing 2% FCS and 0.1% sodium azide. Subsequent flow cytometric analysis was performed on a FACScan (Becton Dickinson, Mountain View, CA). Fluorescence data were displayed as dot plots using the Cell Quest software (Becton Dickinson).

Calculation of the fraction of dead cells during a single cell cycle

Assuming that wild-type cells divide every 8 h, the cumulative cell number of wild-type cells increases by $2^{12} \approx 4\times10^3$ in 96 h (12 divisions). This value is close to the observed increase in cell number, i.e. 7×10^3. During the same period, *RAD54*$^{-/-}$ cells expanded by 8×10^2. Taking the length of a single *RAD54*$^{-/-}$ cell cycle as 8 h and the relative increase of *RAD54*$^{-/-}$ cells per cell cycle as x, from $x^{12} = 8\times10^2$, x can be calculated as 1.74. Thus, 13% of *RAD54*$^{-/-}$ cells may die during a single cell cycle.

Flow cytometric analysis to measure dead cells

To determine the proportion of dead cells, cells were resuspended in PBS containing 5 μg/ml PI, and analyzed immediately by FACSCalibur (Becton Dickinson). We used Annexin V apoptosis kit (Clontech) to stain dying cells.

Measurement of surviving colonies following γ- or X-radiation and treatment with MMS

Serially diluted cells were plated in triplicate onto 6-well clusters with 5 ml/well of 1.5% (w/v) methylcellulose (Aldrich, Milwaukee, WI) plates containing D-MEM/F-12 (Gibco-BRL), 15% FCS, 1.5% chicken serum and 10^{-5} M β-mercaptoethanol. Subsequently, γ-radiation of the cells was performed using ^{137}Cs (0.02 Gy/s, Gammacell 40, Atomic Energy of Canada Limited Industrial Products, Ontario, Canada). X-radiation of the cells was performed using 150 kVp X-rays (Softex Co., Tokyo, Japan) operated at 10 mA, 2.0 mm aluminum filtration. To determine sensitivity to the alkylating reagent, MMS (Sigma), serially-diluted cells were plated in MMS-containing methylcellulose plates.

Colonies were counted at 7 days after irradiation or MMS treatment. Percentage survival was determined relative to numbers of colonies from untreated cells.

Synchronization of cells

To measure cell-cycle-phase specific radiation sensitivity, cells were synchronized with nocodazole (Sigma) or centrifugal counterflow elutriation (Beckman, Palo Alto, CA). To enrich cells at prometaphase, cells were cultured in medium containing 0.5 μg/ml nocodazole for 7 h, then washed three times with pre-warmed medium. Four hours after nocodazole treatment, the plating efficiency of each genotype in methylcellulose plates was analyzed. Among the cells treated with nocodazole, ~80% of wild-type and *KU70*$^{-/-}$ cells and ~50% of *RAD54*$^{-/-}$ cells gave rise to colonies, whereas only ~10% of *KU70*$^{-/-}$*RAD54*$^{-/-}$ cells were capable of forming colonies. To enrich cells at G_1 phase by elutriation, ~5×10^8 cells in 100 ml medium containing 1% chicken serum and 10 mM HEPES [*N*-(2-hydroxyethyl)piperazine-*N*′-(4-butanesulfonic acid)] pH 7.2 ('elutriation medium') were loaded at 1.5 ml/min flow rate onto the Sanderson-type chamber rotating at 1400 r.p.m. at 2°C. The rate of counterflow of elutriation medium was increased by 0.5 ml/min every hour, and cells elutriated at a flow rate of 2.5–3.0 ml/min were collected. The number of live cells was measured using flow cytometry as described above. The plating efficiency of wild-type, *KU70*$^{-/-}$ and *RAD54*$^{-/-}$ genotypes was comparable between PI$^-$ elutriated cells and cells cultured under normal conditions. Cells were released into fresh medium, and cultured under ordinary conditions. At the indicated time points following nocodazole treatment or elutriation, cells were irradiated with γ-rays or X-rays, respectively, as described above. At the same time, samples were taken for cell-cycle analysis.

Karyotype analysis

Karyotype analysis was carried out as previously described (Sonoda *et al*., 1998). Briefly, cells were treated for 3 h with medium containing 1 mg/ml colcemid (Gibco-BRL). Harvested cells were incubated in 1 ml 0.9% sodium citrate for 15 min at room temperature and fixed in 5 ml freshly prepared 3:1 mixture of methanol and acetic acid. The cell suspension was dropped onto an ice-cold wet glass slide and immediately flame dried. Slides were stained with 3% Giemsa solution at pH 6.4 for 10 min.

Acknowledgements

We would like to thank Dr T.Mimori for kindly providing human Ku70 cDNA. We would like to thank Drs S.Kondo (Kinki University, Osaka, Japan), T.Shibata (Riken, Wako, Japan), D.van Gent, J.H.J.Hoeijmakers (Erasmus University, Rotterdam), P.Jeggo (Sussex University, Brighton, UK), W.F.Morgan (UCSF, CA), L.H.Thompson (Lawrence Livermore National Laboratory, CA) and J.-M.Buerstedde (University of Hamburg, Germany) for critically reading the manuscript, and M.Hashishin, Y.Sato, O.Koga and M.Hirao for their excellent technical assistance. C.M. is the recipient of a JSPS Postdoctoral Fellowship. The Bayer-chair of the Department of Molecular Immunology and Allergology is supported by Bayer Yakuhin, Kyoto, Japan. This work was supported in part by a Grant-in-Aid for Scientific Research on Priority Areas from the Ministry of Education, Science and Culture of Japan and by a grant from The Mochida Memorial Foundation for Medical and Pharmaceutical Research.

References

Baba,T.W., Giroir,B.P. and Humphries,E.H. (1985) Cell lines derived from avian lymphomas exhibit two distinct phenotypes. *Virology*, **144**, 139–151.

Benjamin,M.B., Potter,H., Yandell,D.W. and Little,J.B. (1991) A system for assaying homologous recombination at the endogenous human thymidine kinase gene. *Proc. Natl Acad. Sci. USA*, **88**, 6652–6656.

Bezzubova,O.Y. and Buerstedde,J.M. (1994) Gene conversion in the chicken immunoglobulin locus: a paradigm of homologous recombination in higher eukaryotes. *Experientia*, **50**, 270–276.

Bezzubova,O., Shinohara,A., Mueller,R.G., Ogawa,H. and Buerstedde,J.M. (1993a) A chicken RAD51 homologue is expressed at high levels in lymphoid and reproductive organs. *Nucleic Acids Res.*, **21**, 1577–1580.

Bezzubova,O.Y., Schmidt,H., Ostermann,K., Heyer,W.D. and Buerstedde,J.M. (1993b) Identification of a chicken RAD52 homologue suggests conservation of the RAD52 recombination pathway throughout the evolution of higher eukaryotes. *Nucleic Acids Res.*, **21**, 5945–5949.

Bezzubova,O.Y., Silbergleit,A., Yamaguchi-Iwai,Y., Takeda,S. and Buerstedde,J.M. (1997) Reduced X-ray resistance and homologous recombination frequencies in a *RAD54*$^{-/-}$ mutant of the chicken DT40 cell line. *Cell*, **89**, 185–193.

Boulton,S.J. and Jackson,S.P. (1996a) Identification of a *Saccharomyces cerevisiae* Ku80 homologue: roles in DNA double strand break rejoining and in telomeric maintenance. *Nucleic Acids Res.*, **24**, 4639–4648.

Boulton,S.J. and Jackson,S.P. (1996b) *Saccharomyces cerevisiae* Ku70 potentiates illegitimate DNA double-strand break repair and serves as a barrier to error-prone DNA repair pathways. *EMBO J.*, **15**, 5093–5103.

Buerstedde,J.M. and Takeda,S. (1991) Increased ratio of targeted to random integration after transfection of chicken B cell lines. *Cell*, **67**, 179–188.

Buerstedde,J.M., Reynaud,C.A., Humphries,E.H., Olson,W., Ewert,D.L. and Weill,J.C. (1990) Light chain gene conversion continues at high rate in an ALV-induced cell line. *EMBO J.*, **9**, 921–927.

Cheong,N., Wang,X., Wang,Y. and Iliakis,G. (1994) Loss of S-phase-dependent radioresistance in irs-1 cells exposed to X-rays. *Mutat. Res.*, **314**, 77–85.

Critchlow,S.E., Bowater,R.P. and Jackson,S.P. (1997) Mammalian DNA double-strand break repair protein XRCC4 interacts with DNA ligase IV. *Curr. Biol.*, **7**, 588–598.

Darroudi,F. and Natarajan,A.T. (1987) Cytological characterization of Chinese hamster ovary X-ray-sensitive mutant cells, xrs 5 and xrs 6. II. Induction of sister-chromatid exchanges and chromosomal aberrations by X-rays and UV-irradiation and their modulation by inhibitors of poly (ADP-ribose) synthetase and α-polymerase. *Mutat. Res.*, **177**, 149–160.

Essers,J., Hendriks,R.W., Swagemakers,S.M.A., Troelstra,C., de Wit,J., Bootsma,D., Hoeijmakers,J.H.J. and Kanaar,R. (1997) Disruption of mouse RAD54 reduces ionizing radiation resistance and homologous recombination. *Cell*, **89**, 195–204.

Feldmann,H. and Winnacker,E.L. (1993) A putative homologue of the human autoantigen Ku from *Saccharomyces cerevisiae*. *J. Biol. Chem.*, **268**, 12895–12900.

Fingerhut,R., Kiefer,J. and Otto,F. (1984) Cell cycle parameters in radiation sensitive strains of *Saccharomyces cerevisiae*. *Mol. Gen. Genet.*, **193**, 192–194.

Game,J.C. (1993) DNA double-strand breaks and the *RAD50–RAD57* genes in *Saccharomyces*. *Semin. Cancer Biol.*, **4**, 73–83.

Game,J.C. and Mortimer,R.K. (1974) A genetic study of X-ray sensitive mutants in yeast. *Mutat. Res.*, **24**, 281–292.

Gecz,J., Pollard,H., Consalez,G., Villard,L., Stayton,C., Millasseau,P., Khrestchatisky,M. and Fontes,M. (1994) Cloning and expression of the murine homologue of a putative human X-linked nuclear protein gene closely linked to PGK1 in Xq13.3. *Hum. Mol. Genet.*, **3**, 39–44.

Godwin,A.R., Bollag,R.J., Christie,D.M. and Liskay,R.M. (1994) Spontaneous and restriction enzyme-induced chromosomal recombination in mammalian cells. *Proc. Natl Acad. Sci. USA*, **91**, 12554–12558.

Grawunder,U., Wilm,M., Wu,X., Kulesza,P., Wilson,T.E., Mann,M. and Lieber,M.R. (1997) Activity of DNA ligase IV stimulated by complex formation with XRCC4 protein in mammalian cells. *Nature*, **388**, 492–495.

Gu,Y., Jin,S., Gao,Y., Weaver,D.T. and Alt,F.W. (1997) Ku70-deficient embryonic stem cells have increased ionizing radiosensitivity, defective DNA end-binding activity and inability to support V(D)J recombination. *Proc. Natl Acad. Sci. USA*, **94**, 8076–8081.

Guacci,V., Koshland,D. and Strunnikov,A. (1997) A direct link between sister chromatid cohesion and chromosome condensation revealed through the analysis of MCD1 in *S. cerevisiae*. *Cell*, **91**, 47–57.

ISCN1985 (1985) *An International System for Human Cytogenetic Nomenclature*. Report of the Standing Commitee on Human Cytogenetic Nomenclature. Karger, Basel, Switzerland.

Jeggo,P.A. (1990) Studies on mammalian mutants defective in rejoining double-strand breaks in DNA. *Mutat. Res.*, **239**, 1–16.

Jeggo,P.A. (1997) DNA-PK: at the cross-roads of biochemistry and genetics. *Mutat. Res.*, **384**, 1–14.

Kadyk,L.C. and Hartwell,L.H. (1992) Sister chromatids are preferred over homologs as substrates for recombinational repair in *Saccharomyces cerevisiae*. *Genetics*, **132**, 387–402.

Kanaar,R. *et al.* (1996) Human and mouse homologs of the *Saccharomyces cerevisiae RAD54* DNA repair gene: evidence for functional conservation. *Curr. Biol.*, **6**, 828–838.

Kemp,L.M. and Jeggo,P.A. (1986) Radiation-induced chromosome damage in X-ray-sensitive mutants (xrs) of the Chinese hamster ovary cell line. *Mutat. Res.*, **166**, 255–263.

Kozak,M. (1986) Bifunctional messenger RNAs in eukaryotes. *Cell*, **47**, 481–483.

Kozak,M. (1995) Adherence to the first-AUG rule when a second AUG codon follows closely upon the first. [Published erratum appears in *Proc. Natl Acad. Sci. USA*, **92**, 7134]. *Proc. Natl Acad. Sci. USA*, **92**, 2662–2666.

Lee,S.E., Mitchell,R.A., Cheng,A. and Hendrickson,E.A. (1997) Evidence for DNA-PK-dependent and -independent DNA double-strand break repair pathways in mammalian cells as a function of the cell cycle. *Mol. Cell. Biol.*, **17**, 1425–1433.

Li,Z., Otevrel,T., Gao,Y., Cheng,H.L., Seed,B., Stamato,T.D., Taccioli,G.E. and Alt,F.W. (1995) The XRCC4 gene encodes a novel protein involved in DNA double-strand break repair and V(D)J recombination. *Cell*, **83**, 1079–1089.

Lim,D.-S. and Hasty,P. (1996) A mutation in mouse *rad51* results in an early embryonic lethal that is suppressed by a mutation in *p53*. *Mol. Cell. Biol.*, **16**, 7133–7143.

Liu,N. *et al.* (1998) XRCC2 and XRCC3, new human Rad51-family members, promote chromosome stability and protect against DNA crosslinks and other damages. *Mol. Cell*, **1**, 783–793.

Martin,S.J., Reutelingsperger,C.P., McGahon,A.J., Rader,J.A., van-Schie,R.C., LaFace,D.M. and Green,D.R. (1995) Early redistribution of plasma membrane phosphatidylserine is a general feature of apoptosis regardless of the initiating stimulus: inhibition by overexpression of Bcl-2 and Abl. *J. Exp. Med.*, **182**, 1545–1556.

Michaelis,C., Ciosk,R. and Nasmyth,K. (1997) Cohesins: chromosomal proteins that prevent premature separation of sister chromatids. *Cell*, **91**, 35–45.

Milne,G.T., Jin,S., Shannon,K.B. and Weaver,D.T. (1996) Mutations in two Ku homologs define a DNA end-joining repair pathway in *Saccharomyces cerevisiae*. *Mol. Cell. Biol.*, **16**, 4189–4198.

Mimori,T. and Hardin,J.A. (1986) Mechanism of interaction between Ku protein and DNA. *J. Biol. Chem.*, **261**, 10375–10379.

Mimori,T., Ohosone,Y., Hama,N., Suwa,A., Akizuki,M., Homma,M., Griffith,A.J. and Hardin,J.A. (1990) Isolation and characterization of cDNA encoding the 80-kDa subunit protein of the human autoantigen Ku (p70/p80) recognized by autoantibodies from patients with scleroderma-polymyositis overlap syndrome. *Proc. Natl Acad. Sci. USA*, **87**, 1777–1781.

Mizuta,R., Lasalle,J.M., Cheng,H.-L., Shinohara,A., Ogawa,H., Copeland,N., Jenkins,N.A., Lalande,M. and Alt,F.W. (1997) RAB22 and RAB163/mouse BRCA2: proteins that specifically interact with the RAD51 protein. *Proc. Natl Acad. Sci. USA*, **94**, 6927–6932.

Moore,J.K. and Haber,J.E. (1996) Cell cycle and genetic requirements of two pathways of nonhomologous end-joining repair of double-strand breaks in *Saccharomyces cerevisiae*. *Mol. Cell. Biol.*, **16**, 2164–2173.

Morita,T., Yoshimura,Y., Yamamoto,A., Murata,K., Mori,M., Yamamoto,H. and Matsushiro,A. (1993) A mouse homolog of the *Escherichia coli recA* and *Saccharomyces cerevisiae RAD51* genes. *Proc. Natl Acad. Sci. USA*, **90**, 6577–6580.

Moynahan,M.E. and Jasin,M. (1997) Loss of heterozygosity induced by a chromosomal double-strand break. *Proc. Natl Acad. Sci. USA*, **94**, 8988–8993.

Muris,D.F., Vreeken,K., Carr,A.M., Broughton,B.C., Lehmann,A.R., Lohman,P.H. and Pastink,A. (1993) Cloning the RAD51 homologue of *Schizosaccharomyces pombe*. *Nucleic Acids Res.*, **21**, 4586–4591.

Muris,D.F.R., Vreeken,K., Carr,A.M., Murray,J.M., Smit,C., Lohman,P.H.M. and Pastink,A. (1996) Isolation of the *Schizosaccharomyces pombe RAD54* homologue, *rhp54*+, a gene involved in the repair of radiation damage and replication fidelity. *J. Cell Sci.*, **109**, 73–81.

Nussenzweig,A., Chen,C., da-Costa-Soares,V., Sanchez,M., Sokol,K., Nussenzweig,M.C. and Li,G.C. (1996) Requirement for Ku80 in growth and immunoglobulin V(D)J recombination. *Nature*, **382**, 551–555.

Ouyang,H. *et al.* (1997) Ku70 is required for DNA repair but not for T cell receptor gene recombination in vivo. *J. Exp. Med.*, **186**, 921–929.

Petes,T.D., Malone,R.E. and Symington,L.S. (1991) The molecular and cellular biology of the yeast *Saccharomyces*. In Broach,J.R., Pringle,J.R. and Jones,E.W. (eds), *Recombination in Yeast*. Vol. 1. Cold Spring Harbor Laboratory Press, Cold Spring Harbor, NY, pp. 407–522.

Rijkers,T., van den Ouweland,J., Morolli,B., Rolink,A.G., Baarends,W.M., Van Sloun,P.P.H., Lohman,P.H.M. and Pastink,A. (1998) Targeted inactivation of *MmRAD52* reduces homologous recombination but not resistance to ionizing radiation. *Mol. Cell. Biol.*, in press.

Saeki,T., Machida,I. and Nakai,S. (1980) Genetic control of diploid recovery after γ-irradiation in the yeast *Saccharomyces cerevisiae*. *Mutat. Res.*, **73**, 251–265.

Savatier,P., Lapillonne,H., van-Grunsven,L.A., Rudkin,B.B. and Samarut,J. (1996) Withdrawal of differentiation inhibitory activity/leukemia inhibitory factor up-regulates D-type cyclins and cyclin-dependent kinase inhibitors in mouse embryonic stem cells. *Oncogene*, **12**, 309–322.

Scully,R., Chen,J., Plug,A., Xiao,Y., Weaver,D., Feunteun,J., Ashley,T. and Livingston,D.M. (1997) Association of BRCA1 with Rad51 in mitotic and meiotic cells. *Cell*, **88**, 265–275.

Sharan,S.K. *et al.* (1997) Embryonic lethality and radiation hypersensitivity mediated by Rad51 in mice lacking Brca2. *Nature*, **386**, 804–810.

Shinohara,A. and Ogawa,T. (1995) Homologous recombination and the roles of double-strand breaks. *Trends Biochem. Sci.*, **20**, 387–391.

Shinohara,A., Ogawa,H., Matsuda,Y., Ushio,N., Ikeo,K. and Ogawa,T. (1993) Cloning of human, mouse and fission yeast recombination genes homologous to *RAD51* and *recA*. [Published erratum appears in *Nature Genet.*, **5**, 312]. *Nature Genet.*, **4**, 239–243.

Smider,V., Rathmell,W.K., Lieber,M.R. and Chu,G. (1994) Restoration of X-ray resistance and V(D)J recombination in mutant cells by Ku cDNA. *Science*, **266**, 288–291.

Sonoda,E., Sasaki,M.S., Buerstedde,J.-M., Bezzubova,O., Shinohara,A., Ogawa,H., Takata,M., Yamaguchi-Iwai,Y. and Takeda,S. (1998) Rad51 deficient vertebrate cells accumulate chromosomal breaks prior to cell death. *EMBO J.*, **17**, 598–608.

Stamato,T.D., Dipatri,A. and Giaccia,A. (1988) Cell-cycle-dependent repair of potentially lethal damage in the XR-1 γ-ray-sensitive Chinese hamster ovary cell. *Radiat. Res.*, **115**, 325–333.

Sturzbecher,H.W., Donzelmann,B., Henning,W., Knippschild,U. and Buchhop,S. (1996) p53 is linked directly to homologous recombination processes via RAD51/RecA protein interaction. *EMBO J.*, **15**, 1992–2002.

Subramani,S. and Seaton,B.L. (1988) Homologous recombination in mitotically dividing mammalian cells. In Kucherlapati,R. and Smith,G.R. (eds), *Genetic Recombination*. American Society for Microbiology, Washington DC, pp. 549–573.

Sugawara,H., Kurosaki,M., Takata,M. and Kurosaki,T. (1997) Genetic evidence for involvement of type 1, type 2 and type 3 inositol 1,4,5-trisphosphate receptors in signal transduction through the B-cell antigen receptor. *EMBO J.*, **16**, 3078–3088.

Taccioli,G.E. *et al.* (1994) Ku80: product of the *XRCC5* gene and its role in DNA repair and V(D)J recombination. *Science*, **265**, 1442–1445.

Takata,M. and Kurosaki,T. (1996) A role for Bruton's tyrosine kinase in B cell antigen receptor-mediated activation of phospholipase C-γ 2. *J. Exp. Med.*, **184**, 31–40.

Takeda,S., Masteller,E.L., Thompson,C.B. and Buerstedde,J.M. (1992) RAG-2 expression is not essential for chicken immunoglobulin gene conversion. *Proc. Natl Acad. Sci. USA*, **89**, 4023–4027.

Tashiro,S., Kotomura,N., Shinohara,A., Tanaka,K., Ueda,K. and Kamada,N. (1996) S phase specific formation of the human Rad51 protein nuclear foci in lymphocytes. *Oncogene*, **12**, 2165–2170.

Teo,S.-H. and Jackson,S.P. (1997) Identification of *Saccharomyces cerevisiae* DNA ligase IV: involvement in DNA double-strand break repair. *EMBO J.*, **16**, 4788–4795.

Thompson,L.H. (1996) Evidence that mammalian cells possess homologous recombinational repair pathways. *Mutat. Res.*, **363**, 77–88.

Tsuzuki,T., Fujii,Y., Sakumi,K., Tominaga,Y., Nakao,K., Sekiguchi,M., Matsushiro,A., Yoshimura,Y. and Morita,T. (1996) Targeted disruption of the *Rad51* gene leads to lethality in embryonic mice. *Proc. Natl Acad. Sci. USA*, **93**, 6236–6240.

Uckun,F.M., Waddick,K.G., Mahajan,S., Jun,X., Takata,M., Bolen,J. and Kurosaki,T. (1996) BTK as a mediator of radiation-induced apoptosis in DT-40 lymphoma B cells. *Science*, **273**, 1096–1100.

Weaver,D.T. (1995) What to do at an end: DNA double-strand-break repair. *Trends Genet.*, **11**, 388–392.

Wilson,T.E., Grawunder,U. and Lieber,M.R. (1997) Yeast DNA ligase IV mediates non-homologous DNA end joining. *Nature*, **388**, 495–498.

Yamaguchi-Iwai,Y., Sonoda,E., Buerstedde,J.-M., Bezzubova,O., Morrison,C., Takata,M., Shinohara,A. and Takeda,S. (1998) Homologous recombination, but not DNA repair, is reduced in vertebrate cells deficient in *RAD52*. *Mol. Cell Biol.*, in press.

Yamamoto,A. *et al.* (1996) Cell cycle-dependent expression of the mouse Rad51 gene in proliferating cells. *Mol. Gen. Genet.*, **251**, 1–12.

Yaneva,M., Kowalewski,T. and Lieber,M.R. (1997) Interaction of DNA-dependent protein kinase with DNA and with Ku: biochemical and atomic-force microscopy studies. *EMBO J.*, **16**, 5098–5112.

Zdzienicka,M.Z. (1995) Mammalian mutants defective in the response to ionizing radiation-induced DNA damage. *Mutat. Res.*, **336**, 203–213.

Zhu,C., Bogue,M.A., Lim,D.S., Hasty,P. and Roth,D.B. (1996) Ku86-deficient mice exhibit severe combined immunodeficiency and defective processing of V(D)J recombination intermediates. *Cell*, **86**, 379–389.

Zou,H. and Rothstein,R. (1997) Holliday junctions accumulate in replication mutants via a RecA homolog-independent mechanism. *Cell*, **90**, 87–96.

Received January 14, 1998; revised July 2, 1998; accepted July 21, 1998